Development of Comparative Reading System Using 1D SOM for Brain Dock Examinations

Kazuhito SATO, *Member, IEEE*, Sakura Kadowaki, Hirokazu Madokoro, *Member, IEEE*, and Atsushi Inugami

***Abstract*— We propose an objective segmentation method for Magnetic Resonance (MR) images of the brain using self-mapping characteristics of one-dimensional Self-Organizing Maps (SOM). The proposed method requires no operators to specify the representative points, but can segment tissues (such as cerebrospinal fluid, gray matter and white matter) needed for diagnosis of brain atrophy. Doing clinical image experiments, we demonstrate the effectiveness of our method. As a result, we can obtain segmentation results that agree with anatomical structures such as continuities and boundaries of brain tissues. In addition, we propose a Computer-Aided Diagnosis (CAD) system for brain dock examinations based on the use case analysis of diagnostic reading, and construct a prototype system for reducing loads to diagnosticians that occur in quantitative analyses of the extent of brain atrophy. Through field tests of 193 examples of brain dock medical examinees at Akita Kumiai General Hospital, we also present the prospect of efficient support of diagnostic reading in the clinical field because the aging situation of brain atrophy is readily quantifiable irrespective of diagnosticians' expertise.**

I. Introduction

With recent progress of modalities such as Magnetic Resonance Imaging (MRI) and X-ray Computed Tomography (CT), a large amount of high-resolution medical images have been produced at clinical sites. These medical images fulfil a large role for diagnosis of various diseases. Images obtained by MRI clearly depict soft tissues. For that reason, MR images have served as an important information source for image diagnosis of head areas, the abdominal region, etc. Brain matter, as assessed by MRI, can generally be categorized as White Matter (WM), Gray Matter (GM), cerebrospinal fluid (CSF), or vasculature. Most brain structures are defined anatomically according to boundaries of these tissue classes. Therefore, a method to segment tissues into these categories is an important step in quantitative brain morphology. For example, in relation to brain dock examinations, which have become more common recently in Japan, diagnosticians have diagnosed the existence of brain diseases (brain tumor, cerebral hemorrhage, cerebral infarction, etc.) using MR images of several decade slices obtained under different conditions. Because MR image characteristics are very complicated, diagnosticians in clinical fields cannot sufficiently utilize the information of MR images. Actual cases of such misunderstandings of the meanings of categorized tissues have arisen [1].

Comparative readings were performed to diagnose newly generated lesions and the time-dependent change of known lesions, but the danger remains of overlooking lesions that overlap with normal structures [2]. After adjusting the registration of images obtained on different days, studies investigating processing of the different image intensity values have also been attempted. Nevertheless, that process presents the problem in which a false image is generated because of image registration mismatches in details and changes of intensity based on interpolating image positions [3]. With a working group that examined variation of diagnostic reading abilities within numerous physicians' clinical facilities, large variation was found among diagnoses using cerebral blood flow Single Photon Emission Computed Tomography (SPECT). The accuracy of diagnostic reading of MRI is inferior to SPECT, and as dispersive factors, experiences in diagnostic reading and difficulties for differentiation have both been reported [4].

Reports of Computer-Aided Diagnosis (CAD) using MR brain images include only the following studies: a detection method of the lacunar region using T2-weighted images proposed by Yokoyama et al. [5], automated extraction of brain tissues by Tada et al. [6], and extraction boundaries of brain tumors using a three-dimensional region expansion scheme by Ueno et al. [7]. Most segmentation techniques have relied on multi-spectral characteristics of the MR images, although a few studies have reported segmentation from single-channel images. In many clinical applications, it is important to classify tissues only from single-channel MR images [8]. By segmenting brain tissues into separate regions for diagnosis such as the extraction of objective organ and disease region, the development of new application technologies is anticipated. However, these remain dependent on manual designations. Even with the recent progress of computer image analysis techniques and MR technology, and considerable interest in clinical studies, an automated method for segmentation of brain tissues remains unavailable for clinical use.

We propose a segmentation method of MR brain images that emphasizes self-mapping characteristics of a one-dimensional (1D) SOM [9]. In addition, we are developing a diagnostic support system as a CAD system for the brain dock. For reducing the load of diagnosticians who analyze, quantitatively, the degree of brain atrophy and lesion area, we propose an image analysis technique based on the 1D

Kazuhito Sato and Hirokazu Madokoro are with the Faculty of Systems Science and Technology, Akita Prefectural University, Yurihonjo-shi, 015-0055, Japan (phone: +81 184 272178; e-mail: ksato@akita-pu.ac.jp). Sakura Kadowaki is with SmartDesign Corp., 3-1-1 Sannou, Akita 010-8572, Japan. Atsushi Inugami is with Akita Kumiai General Hospital, 273-1, Nishibukuro, Iijima, Akita 011-0948, Japan.

SOM of the smallest unit number of 5, which can maintain the neighborhood region. This method has the feature of quantifying them, based only on image characteristics of the diagnostic reading object. Therefore, it is not dependent on the subject of diagnosticians.

II. Use case Analysis of Diagnostic Reading

Although the human brain atrophies with age [10], [11], brain atrophy reportedly correlates not only with aging but also with risk factors of cerebrovascular disorders such as drinking and high blood pressure [12], [13]. In addition, usual aging alteration must be differentiated from unhealthy brain atrophy because numerous deformative diseases co-exist with brain atrophy such as Alzheimer's and Pick's diseases. That is to say, brain atrophy evaluation is an important index of brain image diagnosis. The cerebral parenchyma is composed mainly of WM, with GM. The GM consists of neuronal cell bodies, and the WM consists of nerve fibers. The GM volume decreases with age, but the WM volume does not always decrease with age, because of the change of the blood vessel circumference structure [14]. Therefore, it is required that GM and WM be classified in addition to CSF, which shows the extent of atrophy when brain atrophy is evaluated using image analysis. Nevertheless, it is not easy to evaluate brain atrophy objectively, diagnosticians have been diagnosing it subjectively based on their respective experiences.

Morphological diagnoses of the brain using MRI carry out investigations that evaluate brain atrophy using the region of interest and the representative cross section interactively. Emphases of those methods engender many problems such as the following. The subject comes in for the selection of the cross section used as the region of interest and analysis, and changes in areas outside the setting region are not examined. In addition, much time depends on the analysis: handling numerous data in interactive analyses is not possible. As the most representative tool to analyze the morphological change of the brain automatically, there is Statistical Parametric Mapping (SPM), developed by Friston et al. [15] It is possible for SPM to detect local morphological changes of the brain for research purposes. However, it is difficult to use SPM to carry out sufficient analyses in brain images with the gap depicted in usual clinical situations. Therefore, an image of thin slice thickness (about 1.5 mm) by three-dimensional imaging and interpolation without a gap is required for SPM.

Automatic processing by the simple operation of inputting MR images is very important for use of this method for objective evaluation of brain atrophy in various clinical fields in a setting such as the brain dock. In addition, because of the difference between imaging parameters and strength of the static magnetic field, image quality and signal strength distribution of the MR image change greatly. Therefore, efficiency improvement and optimization of diagnostic reading are required, considering variations among imaging devices and clinical facilities in addition to diagnosticians.

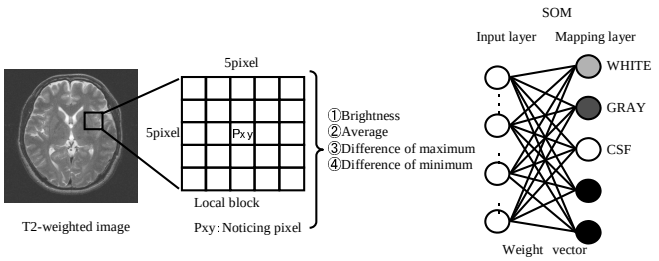

Fig. 2. Segmentation method of brain tissue.

Fig. 1. Brain tissue segmentation method.

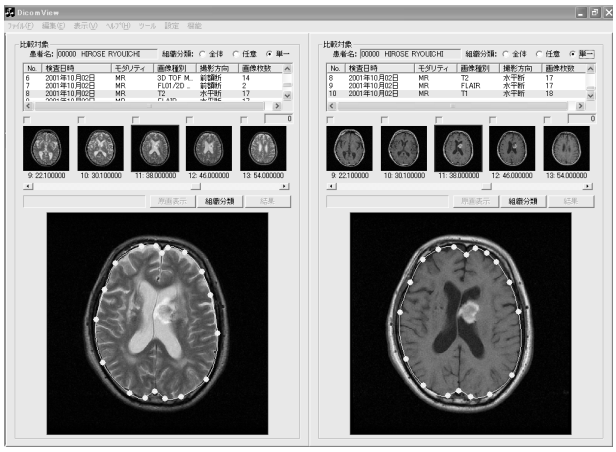

Fig. 2. Window of adjusting the outline to brain surface.

III. Proposed Method

The proposed method requires no specification of representative points by the operator. It segments brain tissues by self-learning of the image properties, such as the brightness distribution, the edge, and the texture information. This method has the feature that regions with obscure boundaries between tissues can be segmented on the basis of topological mapping the feature parameters exhibited in the MR image. The representative index slice was chosen to sample cortical GM, WM, central GM structures, and ventricular CSF.

The procedures are as follows.

STEP 1: Eliminate the scalp and skull regions from the index image in order to obtain the target image for segmentation. We first threshold the gray level image using Otsu's Method [16] based on characteristics of the brightness histogram, and extract the largest object in the threshold image of slice as the target image. Nevertheless, cases exist in which the removal of the skull and scalp region is difficult because of individual differences in brain structure and the delicate change of the image characteristics. In this case, the target brain surface contour is extractable through the smallest interaction with diagnosticians, as shown in Fig. 1. Increase, decrease, and transfer of the nodes forming the contour of the brain surface can be realized through a simple mouse operation; in Fig. 1, these nodes are displayed in the yellow circle.

STEP 2: The pixels under consideration are selected randomly from the target image and the local block is defined

as shown in Fig. 2. As feature parameters of the local block, we calculate the average brightness value of the block, which shows tissue continuity, differences of maximum brightness values and difference of minimum brightness values that give tissue boundaries. The brightness of the pixel under consideration and the calculated feature parameters are input to the SOM to perform self-learning.

STEP 3: After learning, the mapping colors are determined on the basis of the weight vector of the pixel under consideration to the average brightness value given as one feature parameter in the local block. The mapping colors are based on the relative brightness in T2-weighted images of the brain: Among the tissues in T2-weighted images, the CSF is the brightest, followed by the GM, then the WM, and the remainder is least bright. The mapping colors are defined in the above order in accordance with the magnitude of the weight vectors, and the map layer units are labeled.

STEP 4: The brightness values to be mapped are calculated for all pixels in the target image. In determining the mapping value of each pixel, the feature parameters used in learning are input again to the SOM and the winner unit is determined. Then, the brightness value is assigned based on the mapping color that corresponds to the winner unit labeled in STEP3.

IV. Construction of a CAD System for Brain Image

Based on use case analysis of the first diagnostic reading, which concerns preparation of the diagnostic image report, a prototype of the diagnostic image support system, the CAD system for the brain dock, was constructed for use in our proposed method. This CAD system has three characteristic functions: a browsing function for use by the operator; a comparative reading function, which emphasizes relevance to images in the diagnostic reading; and an image analysis function, which maps image characteristics of the diagnostic reading object. This CAD system produces medical images with header information that follows the Digital Image and Communication in Medicine (DICOM) 3.0 standard. It renders all folders and files existing under smartMRI as browsing objects.

A. Browsing Function

The top window of the browsing screen is shown in Fig. 3. Analyses of all header information on the DICOM files (MR brain images) existing under smartMRI are shown in the display window of Fig. 3. The upper part of the browsing window includes the left side in each window of the patient list, study list, and series list. The lower right side of the browsing window is a thumbnail display region. The left side of the lower area is a region that displays the original image chosen in the thumbnail display region. In addition, it is possible to display anterior and posterior slice images of the original image. On the patient list window, a condensed version of patient information as an object is possible simply by selecting the patient age and sex from the menu by adjusting the medical care purpose. The procedure of diagnostic reading is executed by choosing the patient ID first, then choosing the study ID next in the order which searches the series list of an object. In addition, the thumbnail images show slice positions that can be arranged as desired by choosing a series ID that corresponds in the series list. The example depicted in Fig. 3 shows a case in which the axial image of the T2-weighted image was chosen.

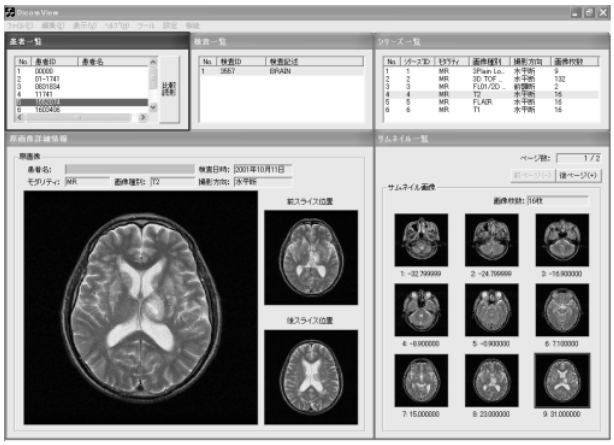

Fig. 3. Browsing window.

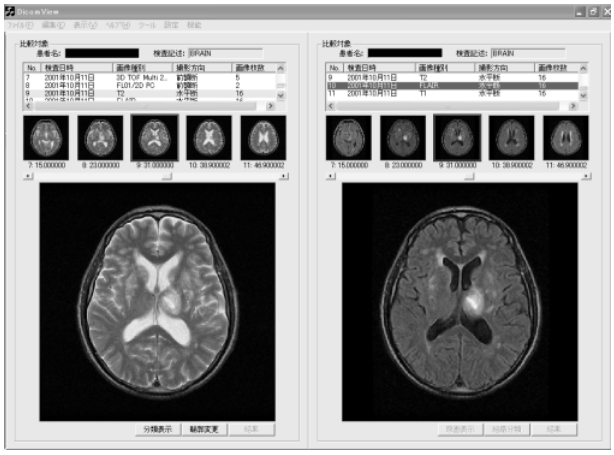

Fig. 4. Window of comparative diagnostic reading.

The original image is expanded and is displayed when the slice image of the attention is chosen in the thumbnail display region. Simultaneously, anterior and posterior slice images are displayed. A change of the slice position can be realized merely by clicking the anterior or posterior slice, while the expanded original image is watched carefully.

B. Comparative Reading Function

Comparative reading is undertaken by choosing the ”comparative reading” menu button of the browsing window. The condition is switched to the comparative reading window in an identical slice cross section (axial, coronal, sagittal) shown in Fig. 4. The left side in the window shown in Fig. 4 is a T2-weighted image. The right side is the FLAIR image. In addition, both images are the same slice position in identical axial. When the object of comparative reading is switched, comparative reading that optionally changes

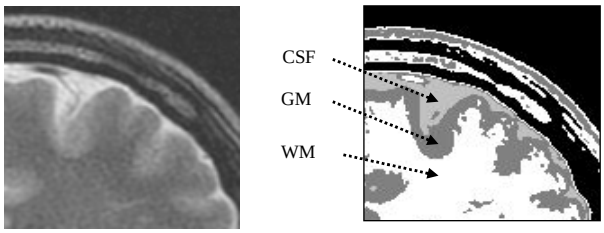

(a) (b)

Fig. 5. Segmentation sample of brain tissue: (a) original image, (b) segmented image.

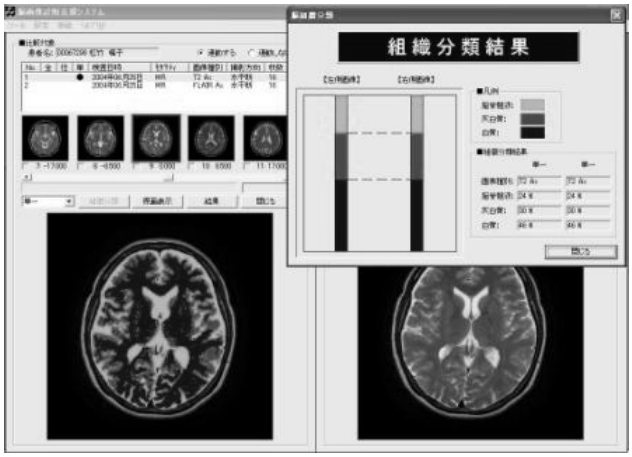

Fig. 6. Case A of diagnostic reading using our proposed method.

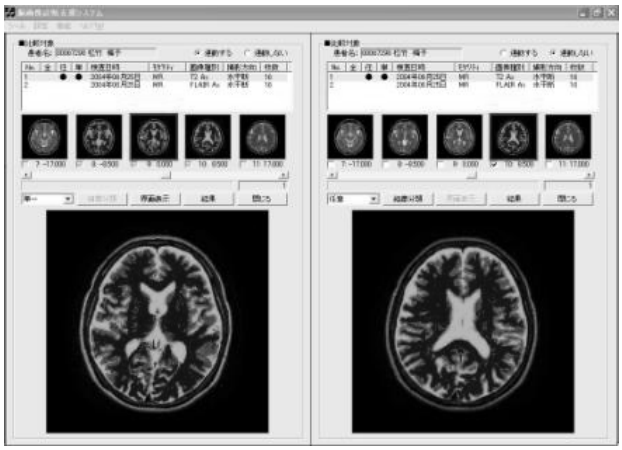

Fig. 7. Case B of diagnostic reading using our proposed method.

TABLE I

DETAILS OF AGE GROUPS AND SEX OF PEOPLE EXAMINED AT THE BRAIN DOCK.

Age-group	Male	Female	Total
30s	2	2	4
40s	30	17	47
50s	78	27	105
60s	22	10	32
70s	3	2	5
Total	135	58	193

image types, slice directions, modality, etc. is possible by choosing a corresponding series ID from the series list, which is displayed respectively in the upper parts of the left window and right window. In addition, the change of the slice position is executed only by clicking thumbnail images displayed under the series list. In addition, slice positions on the right and left change, although they are linked. Therefore, diagnosticians should not feel stress by the need for useless operations such as ordering and rearrangement of images. They can concentrate their attention on the original diagnostic reading.

C. Image Analysis Function

Using features of the image analysis function, the brain tissue of the diagnostic reading object can be classified automatically, merely by learning image characteristics such as edge and brightness distributions. That is to say, intervention of diagnosticians is not required. For application of this image analysis function, extraction of the lesion area in comparative reading and quantification of the brain atrophy with age can be realized because segmentation of the region in which the boundary of brain tissues is unclear becomes possible. In the example of a T2-weighted image shown in Fig. 5, the boundary of the CSF is portrayed as a high brightness region and GM. Regarding the boundary of WM and GM, even if the boundary is indistinct on the original image in the visual observation, the boundaries between tissues can be confirmed clearly in the segmented image.

Diagnostic reading of the analytical result can be executed using the comparative reading function. Fig. 6 is an example showing the original image at the left side and the segmentation result of the brain tissue at the right side in the window. Diagnostic reading is possible, but the validity of the segmentation result is contrasted with the original image. By clicking the graphical representation button, it is possible to obtain the occupation proportion of each tissue in making the intracranial region as 100 percent. Simultaneously, diagnostic reading for multiple slice images is realized by putting a check in the thumbnail image displayed under the series list, as shown in Fig. 7, by totaling the segmentation result of chosen each slice image, and graphing the result. In addition, a general tendency and partial tendency in an axial section of interest can be grasped when shown in comparison to segmentation results of one slice image like that shown at the right side. These segmentation results can be output as a CSV file.

TABLE II

DETAILS OF STANDARD VARIATIONS AMONG AGE GROUPS.

Age-group	Whole Sample(%)	Nomal Samples(%)
30s	1.22	—
40s	1.89	1.63
50s	2.03	1.69
60s	2.57	2.05
70s	2.23	—

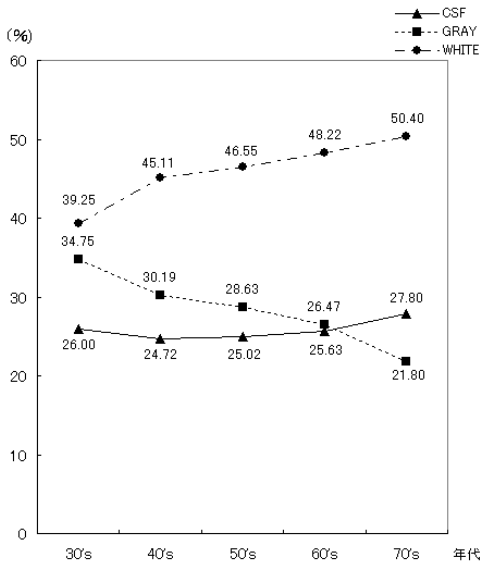

Fig. 8. Overall brain atrophy tendencies with age.

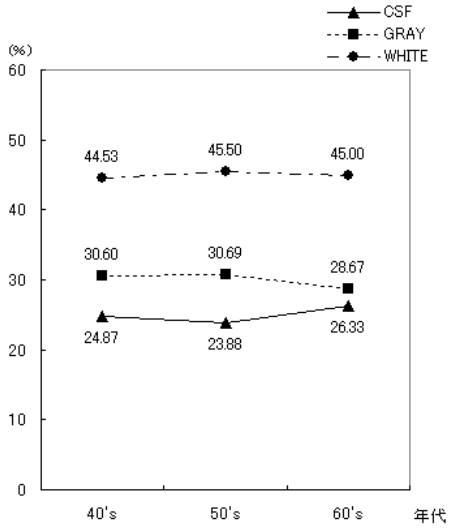

Fig. 9. Brain atrophy tendencies with age among normal people.

V. Field Test

For medical examinees of the brain dock at Akita Kumiai General Hospital, field tests were carried out to assess the effectiveness of this CAD system for diagnostic reading. MR images as a diagnostic reading object are the T2-weighted image and the FLAIR image taken in MRI modality (EXCELART1.5T; Toshiba Medical Systems Corp.). These are all axial images with a slice gap of 6 mm. The T2-weighted image emphasizes the difference in the transversal relaxation time between protons in the tissues. It is used most frequently in the clinical field because it can depict edema and tumors, which have a long transversal relaxation time, with high brightness. The resolution of the MR image is 512 $\times$ 512 pixels; its brightness level is 16 bit.

The evaluation objects are MR images (6324 images) of 193 examples from 135 males and 58 females who had brain-dock medical examinations at Akita Kumiai General Hospital

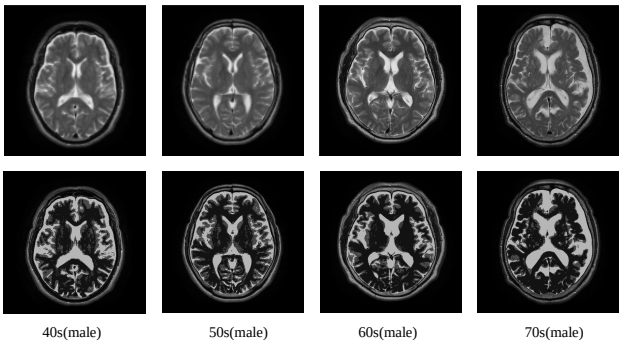

Fig. 10. Segmentation results of representative images in each age group.

during January 2004 through November 2005. These image data sets are acquired in all identical imaging parameters. There is no change of signal strength according to differences of the parameters. Regarding medical examinees of 193 examples, the breakdowns by age and sex are shown in Table I. For all medical examinees of the brain dock, there were 193 examples. The patient group comprising those who were diagnosed with the normal range were 34 examples comprising 23 males and 11 females. We carried out age-independent quantification of atrophy. Results for all medical examinees are shown in Fig. 8; results of patient groups who were diagnosed as within the normal range are shown in Fig. 9. We calculate the standard deviation as a degree of dispersion on the each sample point, and Table II shows the results of arranging them.

In Fig. 8, the proportion generally increases with age. The CSF space showing the degree of atrophy, and especially, the tendency is remarkable in the 70s. For the 40s and 50s cadres of examinees, although the value of the standard deviation showing a variation of individual specificity is small, in the 60s and 70s cadres, the values are large. Although atrophy progresses slowly to middle age (30s–50s), individual specificity is not recognized. In contrast, there is marked individual specificity in later progress of atrophy with age (60s, 70s). A clear reference is not possible because a difference exists in number of samples in each generation. Especially few are the samples (five examples) of people in their 70s. However, it can be estimated as the age period in which the remarkable progress of atrophy appears with aging. In other words, by recommending and strictly carrying out brain dock medical examinations of persons over 60, for whom the progress of atrophy is remarkable, it can be expected that the tendency of general atrophy with aging is related to individual specificity because comparative readings for time series image sets of each medical examinee become possible.

On the other hand, as shown by a comparison of Fig. 9 with Fig. 8, the standard deviation value in each generation is small, and the proportion of CSF in the middle age (30s–50s) stabilizes at a low value. In addition, a breakdown of the patient group diagnosed with the normal range are analyzed, and the number of samples of the middle age can be ensured,

such as one examinee in the 30s, 15 examinees in their 40s, and 16 in their 50s. In contrast, the number of samples decreases sharply with the progress of aging: three examples of examinees in their 60s on and none in their 70s. As one reason, it is mentioned that cases diagnosed as asymptomatic cerebral infarction (lacunar infarcts) increase with age.

In an aging society like Japan's, most medical examinees have lifestyle illnesses as a background. Especially, preventive measures against cerebrovascular disorders become important for people diagnosed with hypertension, hyperlipidemia, diabetes, cardiac diseases, etc. By stimulating improvement in lifestyle habits that are closely related to asymptomatic cerebral infarction (lacunar infarct), subsequent symptomatic cerebral infarction might be prevented. Consequently, as shown in Fig. 8, the tendency toward atrophy with age engenders a quantitatively useful guideline in diagnostic image interpretation.

The representative original images and the segmentation results in each generation are shown in Fig. 10. As might be apparent from Fig. 10, the CSF is extracted correctly along the high brightness region on the original image, and the GM forms the banded region along the boundary between the WM and the CSF. These are segmentation results that agree with the anatomical structures of the brain. Furthermore, the segmentation results agree with the anatomical knowledge that the brain atrophy concurs with the extension of third ventricle and lateral ventricle. From the viewpoint of a diagnostician who evaluated the validity of the segmentation results, the following opinions were issued. Extremely interesting functions are diagnostic reading in direct comparison to the segmentation results of respective tissues with the original image. Also interesting is the mechanism that links the observed slice position in the left and right windows, when necessary.

VI. Conclusion

This CAD system for brain dock examinations based on use case analysis of the diagnostic reading was proposed for aiding medical specialists in quantitatively analyzing the degree of brain atrophy. A prototype system was developed. Utilizing a browsing function and a comparative reading function that this CAD system offers, the system can demonstrably support diagnostic reading in the clinical field. A field test for 193 diagnostic examples of brain dock medical examinees at Akita Kumiai General Hospital clarified the progressive tendencies of brain atrophy with aging. The following points represent salient conclusions of this study.

1) The proportion of CSF, showing the degree of atrophy that occurs with aging, increased. Particularly during examinees' seventh decade, that tendency was remarkable.
2) In the examinees' 40s and 50s, the standard deviation, representing the variation of individual specificity, was small. The value was great for examinees in their 60s and 70s.

No great difference was apparent, according to individual specificity, among examinees of the middle age (30s–50s), who typically showed only slight progress of the atrophy. Clear individual specificity existed was apparent for older people (60s, 70s), who showed a progressive tendency of atrophy. Future systems' image analysis functions must be improved for automatic detection of asymptomatic cerebral infarction (lacunar infarcts) that are mainly diagnosed to brain dock medical examinees. In addition, field tests must be conducted continually.

Acknowledgment

This study was conducted as a part of the Collaboration of Regional Entities for the Advancement of Technological Excellence from the Japan Science and Technology Agency (JST) and the Ministry of Education, Culture, Sports, Science and Technology of Japan.

References

[1] H. Fukatsu, "Special edition paper - The Expectation to the Medical Image Engineering from the Viewpoint of Diagnostic Reading Doctor-MRI," *Medical Imaging Technology,* vol. 20, no. 5, pp. 545-550, 2002.
[2] R. E. Greene, "Missed lung nodules Lost opportunities for cancer cure, " *Radiology,* vol. 182, pp. 8-9, 1992.
[3] A. Kano, K. Doi, H. MacMahon, et al., "Digital image subtraction of temporally sequential chest images for detection of interval change," *Med. Phys,* vol. 21(3), pp. 435-461, 1994.
[4] K. Machida, et al., "The Comparison of Cerebral Blood Flow SPECT and Dementia Diagnosability of the MRI and the Examination of the Fluctuation of Diagnostic Reading Ability Between Diagnostic Reading Doctors in Multiple Facilities," Workgroup Report in the Heisei 13 Fiscal Year.
[5] R. Yokoyama, T. Hara, et al., "The Trial of the Automatic Detection of the Lacunar Infarction Region in the Brain MRI," *Japanese Journal of Radiological Technology,* vol. 58, no. 3, pp. 399-405, 2002.
[6] Y. Tada, S. Fukunishi, "The Automatic Extraction of the Brain Tissue in MRI Tomography," *The Japan Society of Mechanical Engineers Lecture Proceedings,* no. 97-72, pp. 491-492, 1998.
[7] I. Ueno, T. Fujiwara, K. Matsuda, et al., "Tumor Region Extraction from the Brain MRI using the 3-D Region Expanding Scheme," *IEICE Technical Report,* vol. MI2002-73, pp. 23-28, 2002.
[8] J. C. Rajapakse, J. N. Giedd, and J. L. Rapoport, "Statistical Approach to Segmentation of Single-Channel Cerebral MR Images," *IEEE Trans. Med. Imaging,* vol. 16, no. 2, pp. 176-186, 1997.
[9] T. Kohonen, Self-organizing maps, Springer Series in Information Sciences, 1995.
[10] K. Sato, K. Sugawara, Y. Narita, and I. Nomura, "Consideration of the Method of Image Diagnosis with Respect to Frontal Lobe Atrophy," *IEEE Trans. Nucl. Sci.,* vol. 43, no. 6, pp. 3230-3238, Dec. 1996.
[11] M. Ozkan, B. M. Dawant, and R. J. Maciunas, "Neural Network-Based Segmentation of Multi-Model Medical Images: A Comparative and Prospective Study," *IEEE Trans. Med. Imag.,* vol. 12, no. 3, pp. 534-544, Sep. 1993.
[12] W. E. Reddick, J. O. Glass, E. N. Cook, T. D. Elkin, and R. J. Deaton, "Automated Segmentation and Classification of Multispectral Magnetic Resonance Images of Brain using Artificial Neural Networks," *IEEE Trans. Med. Imaging,* vol. 16, no. 6, pp. 911-918, 1997.
[13] J. Alirezac, M. E. Jernigan, and C. Nahmias, "Automatic segmentation of MR images using self organizing feature mapping and neural networks," *Proceedings of the SPIE The International Society for Optical Engineering,* pp. 138-149, 1997.
[14] R. Sammouda, N. Niki, and H. Nishitani, "Segmentation of Brain MR Images Based on Neural Networks," *IEICE Trans. Inf. & Syst.,* vol. E79-D, no. 4, pp. 349-356, Apr. 1996.
[15] R. Sammouda, N. Niki, and H. Nishitani, "A Comparison of Hopfield Neural Network and Boltzmann Machine in Segmenting MR Images of the Brain," *IEEE Trans. Nucl. Sci.,* vol. 43, no. 6, pp. 3361-3369, Dec. 1996.
[16] N. Otsu, "The Automatic Threshold Selecting Method Based on the Discriminant and the Least Squares Standard," *IEICE(D),* vol. J63-D, no. 4, pp. 349-356, 1980.